

EFFICIENT HIGH-PERFORMANCE BARK-SCALE NEURAL NETWORK FOR RESIDUAL ECHO AND NOISE SUPPRESSION

Ernst Seidel*, Pejman Mowlae^o, Tim Fingscheidt*

*Institute for Communications Technology, Technische Universität Braunschweig
Schleinitzstraße 22, 38106 Braunschweig, Germany
^oGN Audio A/S, Lautrupbjerg 7, 2750 Ballerup, Denmark

ABSTRACT

In recent years, the introduction of neural networks (NNs) into the field of speech enhancement has brought significant improvements. However, many of the proposed methods are quite demanding in terms of computational complexity and memory footprint. For the application in dedicated communication devices, such as speakerphones, hands-free car systems, or smartphones, efficiency plays a major role along with performance. In this context, we present an efficient, high-performance hybrid joint acoustic echo control and noise suppression system, whereby our main contribution is the post-filter NN, performing both noise and residual echo suppression. The preservation of nearend speech is improved by a Bark-scale auditory filterbank for the NN postfilter. The proposed hybrid method is benchmarked with state-of-the-art methods and its effectiveness is demonstrated on the ICASSP 2023 AEC Challenge blind test set. We demonstrate that it offers high-quality nearend speech preservation during both double-talk and nearend speech conditions. At the same time, it is capable of efficient removal of echo leaks, achieving a comparable performance to already small state-of-the-art models such as the end-to-end DeepVQE-S, while requiring only around 10% of its computational complexity. This makes it easily realtime implementable on a speakerphone device.

Index Terms— speech enhancement, acoustic echo control, deep neural network, residual echo suppression, noise reduction.

1. INTRODUCTION

Echo and background noise are major obstacles in everyday life's speech communication. To enable high-quality speakerphones or video conference solutions, a reliable and efficient joint denoising and acoustic echo control solution is strictly required. In particular, as a remaining major challenge for speech communication devices used in real-life, double-talk performance has been often reported as a limiting factor, as the device shall allow users to speak and hear simultaneously without interruptions. Furthermore, a reduced double-talk performance was shown to impair meeting inclusiveness and participation rate [1].

Recently, there has been quite some interest towards deep learning-based solutions for acoustic echo control. Various methods relying on a neural network (NN) have also been proposed for the task of joint denoising and echo cancellation. They can be categorized into two groups: (1) *Fully learned methods*, which describe either a two-stage NN approach with a dedicated acoustic echo control module and a second noise and residual echo suppression (RES) module [2–6], or a single NN trained for a joint task, as an example dereverberation, denoising and echo cancellation (see, e.g., [7–11]). (2) *Hybrid methods* are themselves grouped into two categories:

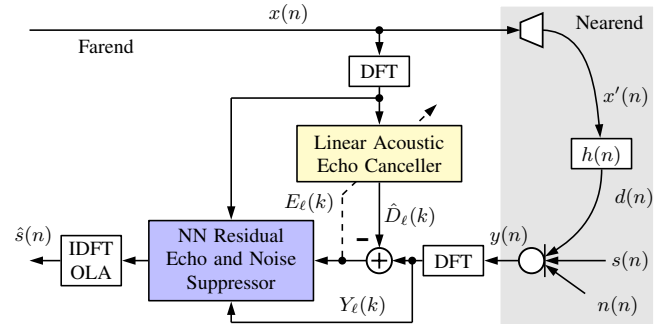


Fig. 1. Hybrid system consisting of a linear acoustic echo canceller and the proposed neural postfilter performing residual echo and noise suppression, details are shown in Fig. 2.

(i) a combined linear echo canceller (LEC) [12, 13] followed by an NN postfilter (PF) as residual echo and/or noise suppressor [14–17], or (ii) an NN-aided step-size control or state estimation for the LEC [18, 19].

Major contributions to the advancement of NN-based acoustic echo control have been the Acoustic Echo Cancellation Challenges organized by Microsoft [20]. Top-performing methods have been reported at these challenges, but their footprints and performance vs. complexity trade-offs are often not allowing for implementation in consumer devices, e.g., a speakerphone or a car's handsfree system.

The recent challenges furthermore revealed that there is still headroom for improving acoustic echo control performance w.r.t. the metrics "double-talk nearend speech preservation" (DT Other) and "single-talk nearend (STNE) MOS" (ST Other) [20]. A possible solution could be the application of an auditory filterbank to imitate the frequency resolution of the human hearing system [17, 21].

Motivated by the above facts and to address the existing challenges, we propose an efficient high-performance NN design for noise and residual echo suppression. The proposed method relies on a classical LEC, which is combined with a low-complexity NN PF incorporating a Bark-scale auditory filterbank. Through various experiments, we demonstrate that the proposed solution offers a good trade-off between echo/noise suppression and near-end speech preservation, while being realtime-capable in a speakerphone device due to its low complexity and memory footprint.

The rest of this paper is organized as follows: In the following Section 2, we present the proposed method and its details. Section 3 elaborates on dataset, training framework, reference methods, and metrics employed in this work. In Section 4, we present the results and discussions. Finally, Section 5 concludes our work.

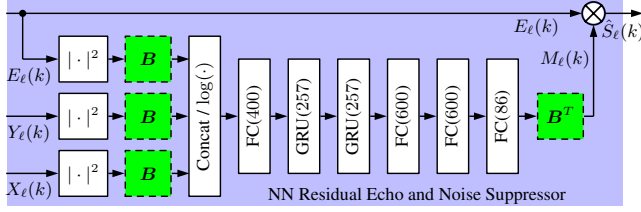


Fig. 2. Neural network architecture of the proposed postfilter shown in Fig. 1, with Bark-scale mapping (green).

2. PROPOSED METHOD

2.1. Problem Formulation

We consider a speakerphone application used for full-duplex communication as shown in Fig. 1. The device has microphone(s) as well as loudspeaker(s) and is located in a room on a table. In this work, we consider a single microphone and loudspeaker, hence the signal received by the microphone is given by:

$$y(n) = s(n) + n(n) + d(n), \quad (1)$$

with $s(n)$ as the (desired) near-end speech signal, $n(n)$ denoting the additive background noise at the near-end, $x(n)$ being the far-end signal, and $d(n) = h(n) * f_{NL}(x(n))$ being the echo. Here, $h(n)$ is the room impulse response (RIR), $f_{NL}(\cdot)$ is the nonlinear function modeling the loudspeaker, and $*$ denotes the convolutional operator.

The problem formulation is as follows: Given the observed microphone signal $y(n)$ and far-end signal $x(n)$, estimate the clean near-end speech signal $s(n)$. With the LEC filter estimate $\hat{h}(n)$, the linear echo component $d(n)$ in the microphone signal is approximated by

$$\hat{d}(n) = x(n) * \hat{h}(n). \quad (2)$$

Subtracting the estimated echo $\hat{D}_\ell(k) = X_\ell(k)\hat{H}_\ell(k)$ in the discrete Fourier transform (DFT) domain, we obtain

$$E_\ell(k) = Y_\ell(k) - X_\ell(k)\hat{H}_\ell(k), \quad (3)$$

where k is the frequency bin index and ℓ the frame index. In a hybrid system, the NN RES and noise suppression stages are trained to find the time-frequency mask $M_\ell(k)$ to be applied on the LEC output $E_\ell(k)$, yielding the final estimate for the clean near-end speech by

$$\hat{S}_\ell(k) = M_\ell(k)E_\ell(k). \quad (4)$$

Using (3), (4), and the DFT of (1), we obtain

$$\hat{S}_\ell(k) = M_\ell(k)S_\ell(k) + M_\ell(k)(N_\ell(k) + \Delta D_\ell(k)), \quad (5)$$

where we defined $\Delta D_\ell(k) = H_\ell(k)X'_\ell(k) - \hat{H}_\ell(k)X_\ell(k)$ and further $x'(n) = f_{NL}(x(n))$ and its DFT as $X'_\ell(k)$. The overall estimation error term defined as $\epsilon_\ell(k) = \hat{S}_\ell(k) - S_\ell(k)$ is then given by

$$\epsilon_\ell(k) = (M_\ell(k) - 1) \cdot S_\ell(k) + M_\ell(k) \cdot (N_\ell(k) + \Delta D_\ell(k)). \quad (6)$$

It can be seen that the error consists of two terms: near-end signal distortion and residual noise and echo error, which itself consists of two components: masked noise and the residual echo due to the remaining non-linear echo not addressed by LEC. The task of the neural network is to estimate the clean near-end speech as its target via minimizing the overall estimation error (6).

2.2. Proposed System

Fig. 1 shows the block diagram for the proposed system, including an LEC block for linear acoustic echo cancellation and an NN postfilter stage. Each stage is described below. The entire model operates (apart from the proposed perceptual mapping) in the DFT domain. To accomplish this, input signals are square-root Hann windowed and the resulting frames are then transformed by a K -point DFT. For synthesis of the output signals, we use another square-root Hann window, K -point IDFT, and overlap-add.

Linear echo canceller: To assure a minimal aliasing level both in-band and across sub-bands, we use an over-sampled filterbank after [22]. For the echo cancellation adaptive algorithm, we employ a subband NLMS filter with joint optimization on both the normalized step-size and regularization parameters [23].

Proposed neural network postfilter: The architecture of the proposed neural network used as postfilter in the hybrid system is shown in Fig. 2. We choose an NSNet2-like architecture [24], which we consider to be a good balance between achievable performance and computational complexity of the solution. It consists of fully connected (FC) and gated recurrent unit (GRU) layers. Motivated from psycho-acoustics and perceptual relevance of log-Bark power spectral features, we apply a mapping from DFT into Bark domain, denoted by the $K \times B$ matrix $\mathbf{B} = (B(k, b))$, applied on the DFT power spectra of the inputs ($|E_\ell(k)|^2, |Y_\ell(k)|^2, |X_\ell(k)|^2$). The output of the filter with input $X_\ell(k)$ is then given by $Z_\ell(b) = \sum_{k \in \mathcal{K}} B(k, b)|X_\ell(k)|^2$, with $k \in \mathcal{K} = [0, K-1]$, where $B(k, b)$ is the b th filter computed within the frequency bin range between $f_l(b)$ and $f_u(b)$, which refer to the starting and end band edges in frequency for the b th filter. For the b th frequency band, the contribution from the energy in the k th DFT bin is given by [25]:

$$B(k, b) = \frac{\max[0, \min(f_u(b), \frac{(2k+1)f_s}{2K}) - \max(f_l(b), \frac{(2k-1)f_s}{2K})]}{f_s/K} \quad (7)$$

where f_s is the sampling rate. We design auditory-motivated filters following the Bark scale to uniformly divide the frequency bin range $k \in \mathcal{K}$ into a number of B bands. Finally, these mapped features are concatenated and compressed by a logarithm before passing them to the first FC layer. After returning from the mapped domain using the transpose of the mapping matrix (\mathbf{B}^T), the NN yields a real-valued mask $M_\ell(k)$.

Loss function: As training loss, we employ the spectral complex compressed mean-squared error (CCMSE) [26] that combines magnitude and phase-aware terms according to

$$J^{\text{CCMSE}} = \sum_{k, \ell} (1 - \alpha) \left| |\tilde{S}_\ell(k)|^c - |S_\ell(k)|^c \right|^2 + \alpha \left| |\tilde{S}_\ell(k)|^c e^{j\varphi_{\tilde{S}}(\ell, k)} - |S_\ell(k)|^c e^{j\varphi_S(\ell, k)} \right|^2, \quad (8)$$

where $0 < \alpha < 1$ is a weighting factor between the two terms, $c = 0.3$, and $\tilde{S}_\ell(k)$ is obtained from sequence $\hat{s}(n)$, again square-root Hann windowing, and DFT (known as short-term Fourier transform consistency enforcement [27]).

3. TRAINING AND EVALUATION FRAMEWORK

3.1. Datasets and Augmentation

Training set: As speech material for $s(n)$ and $x(n)$ we use data provided within the Microsoft Acoustic Echo Cancellation Challenge 2023, consisting of 50,000 recordings from 10,000 environments,

recorded by Mechanical Turk users [20]. We create training signals of 10 s length. As background noise $n(n)$, we include noise files from the training dataset of the ICASSP 2023 Deep Noise Suppression Challenge [28]. Noises are added to the speech at signal-to-noise ratios uniformly distributed with $\text{SNR} \sim \mathcal{U}[0, 30]$ dB. We use a pool of simulated and real RIRs, with various room configurations and isotropic and point-source noises [29]. A random silent period of up to 10 s is included for nearend, echo, and noise to add more realism towards the dynamics of a dialogue in a meeting.

To account for non-linearities of the loudspeaker [30], 80% of the files of $x'(n)$ include $f_{\text{NL}}(x(n))$ either as error function $x'(n) = \eta^{-1} \text{erfc}(\eta \cdot x(n))$ with $\eta = 1$, or as a scaled version ($0 < \eta < 1$ if $x(n) < 0$, else $\eta = 1$) with $\eta \sim \mathcal{U}[-12, 0]$ dB, applied to the negative parts of the reference signal $x(n)$ to reflect the non-linearities of the transducer in a product. The echo $d(n)$ is added with a signal-to-echo ratio $\text{SER} \sim \mathcal{U}[-30, 10]$ dB. As the original data is all fullband, we choose 32-bit linear PCM when writing the audio files. We convert the sampling frequency of all data to 16 kHz. To simulate clock drifts due to resampling, we consider a 1% drift of the device's nominal sampling rate. We augment the echo signal generation with cross-fading between two RIRs. To simulate close distance between speaker and microphone as well as volume change, the second RIR is adjusted in its direct path energy via a gain following a standard deviation of $\sigma = 1.0$ as dynamic RIR mixing gain, and then added to the first RIR. Random bandpass filtering is applied on signal components to reflect the device's frequency response and any mismatch in the device.

Test set: The ICASSP 2023 AEC Challenge blind test set [20] is used to evaluate the performance of the methods studied in this work. It consists of 800 real-world clips with 300 double-talk (DT), 300 single-talk fared (STFE), and 200 single-talk nearend (STNE) examples. The audio files are of variable length, ranging between 30 to 45 seconds. They cover a large variety of distortion types, including strong speaker/mic distortions, stationary/non-stationary noise, glitches resulting in chippy audio, varying gain during the recording, and a cascade effect due to audio processing of the device being active. Please note that the STFE subset of the blind test set consists of very difficult delay estimation cases—either long or variable delays aside from non-linear distortions and stationary noise scenarios [20]. However, as the delay between the mic and loudspeaker mounted on the same device is a known parameter, such long-delay and variable jitter conditions are no typical use case for a speakerphone's echo control processing, hence they are not the main focus for our target application in this study. Accordingly, to exclude the impact of the existing jitter/delay between the fared signal and mic signal in the test set, we performed offline delay compensation of the test data, using cross-correlation between $y(n)$ and $x(n)$.

3.2. Training Setup

As LEC we use the normalized least mean-squares (NLMS) method implemented with an over-sampled filterbank [16]. A sampling rate of 16 kHz, window length of 1024 samples, DFT size of $K = 512$ samples, and a frame shift of 128 samples are used with the prototype filter designed as proposed in [22]. Four filter lengths of $N_{\text{LEC}} \in \{4, 8, 16, 32\}$ taps are considered to address both fast and slow reactions to echo path changes common in realistic conditions as well as to adjust the adaptation speed as a function of the adaptive filter length accordingly. To achieve a better generalization and performance of the LEC stage on mismatched test sets, we allowed LEC parameters to vary randomly in training [14]; namely both, adaptive filter lengths and the smoothing coefficient $\beta \sim \mathcal{U}[0.5, 2]$

for PSD estimation, as factor variation. Motivated from perceptual audio coding and perceptual audio measurement, the postfilter Bark scale is chosen to decompose DFT bins into $B = 86$ uniformly spaced bands on the Bark scale covering a frequency range of 0 Hz to 8 kHz (for design details, we refer the reader to [25]).

Network Training: We initialize the learning rate to 10^{-4} , which drops by a factor of 0.5 once the validation metric does not improve for 10 epochs. We trained the models with 400 epochs, whereby one training epoch comprises 95,000 sequences. For gradient calculation, the Adam optimizer [31] is used in its standard configuration. All models are implemented and trained using PyTorch.

3.3. Reference Methods

As reference methods, we consider the following methods: (i) LEC stage-only, (ii) the fully data-driven DTLN model¹ [10] with 4 consecutive LSTM layers with 256 units each, followed by a fully connected layer with sigmoid activation function, and (iii) the recently proposed efficient DeepVQE-S [7] (denoted as DVQE-S) as the state of the art used in Microsoft Teams², and finally, (iv) we include the results obtained by our proposed method without perceptual mapping **B**, i.e., DFT log-power features as inputs following exactly the same NN topology shown in Fig. 2, loss function, and consistency. This will highlight the impact of the proposed perceptual mapping used in the proposed model.

3.4. Evaluation Metrics

For the instrumental evaluation, we mainly use the AECMOS metric, a non-intrusive, model-based echo cancellation quality predictor [32]. AECMOS individually evaluates echo suppression effectiveness and the effects of other degradations (e.g., noise, nearend degradation). Both measures are reported for DT condition (labeled DT Echo and DT Other). In the STFE condition, only ST Echo is considered. Here, we also report the average logarithmic echo return loss enhancement (ERLE) [33], given by $\text{ERLE} = 10 \log_{10} (\|y(n)\|_2^2 / \|\hat{s}(n)\|_2^2)$, which measures the echo reduction between the unprocessed and enhanced signals when only noise and fared signal are present. Finally, to evaluate the denoising capacity of the methods in the STNE condition, we use ST Other and the DNSMOS metrics, following ITU-T P.835, focused on speech distortion (SIG), background noise attenuation (BAK), and overall quality (OVRL) [34].

4. RESULTS AND DISCUSSION

AECMOS and DNSMOS results: We report the averaged instrumental objective measures of AECMOS and DNSMOS obtained for the three conditions (DT, STFE, STNE) of our test set described in Section 3.1. The results are shown in Fig. 3. We can see that the proposed Bark-scaled hybrid solution yields an overall improvement over the LEC performance in all conditions predicted by AECMOS, except from near-end quality (DT Other), where (a) LEC expectedly scores the highest of all models. Moreover, the comparison against

¹Retrained on our own training data.

²Here, our own implementation is retrained on our training data. Note that in our reference DVQE-S model, we drop the self-attention layer for signal alignment, but rather focus on evaluation of the architecture used for echo control, allowing to demonstrate the achievable performance of the neural network architectures and not its ability to solve the delay compensation or synchronization as detailed in [7–9].

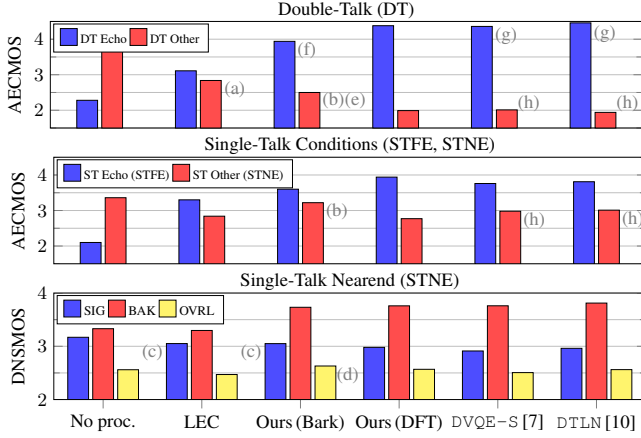


Fig. 3. (Top) AECMOS measurements for the **DT** condition, (middle) ST Echo for the **STFE** and ST Other for the **STNE** condition, (bottom) DNSMOS (SIG/BAK/OVRL) reported for the **STNE** condition. The labels (a) to (h) refer to the discussion below.

our reference model without Bark transformation shows (b) the immense benefits of the perceptually motivated mapping for nearend speech preservation (DT/ST Other). In STNE, our proposed model shows (c) no degradation of SIG when compared to the LEC stage and (d) the highest OVRL score. For the double-talk condition, all the methods offer a trade-off between near-end speech quality (DT Other) and echo removal (DT Echo). Apart from the LEC, our Bark-scale method offers (e) the highest DT Other at the expense of (f) a reduced, but still high DT Echo. The (g) good echo removal offered by our reference models comes at the cost of (h) a noticeably worse nearend speech quality in both double-talk (DT Other) and STNE conditions (ST Other). *All in all, we can conclude that our hybrid proposal keeps state-of-the-art model performance and, through the use of an auditory filterbank, is even capable of achieving a more favorable trade-off regarding nearend speech quality.*

Echo Return Loss Enhancement: We further report the echo control and noise reduction performance in STFE condition measured by the ERLE scores, shown in Table 1. We can see that our proposed NN postfilter significantly improves the echo suppression level achieved by its LEC stage. The DTLN model achieves the highest ERLE, followed by our DFT and Bark models, which score comparably despite their strong performance differences reported in Fig. 3. DVQE-S scores significantly lower. Comparing Fig. 3 and Table 1, we observe that ERLE and ST Echo do not deliver the same rank orders among the methods, e.g., our proposed Bark-scale model scores significantly higher in ERLE than DVQE-S despite having a comparable ST Echo score. We associate this observation to the fact that ST Echo reflects the subjective impression about echo removal [35], while ERLE simply measures the residual signal’s energy. AECMOS might overlook residual echo if it is no longer speech-like, as the underlying NN was trained on subjective listening tests, where noise-like residual echo would be rated as less annoying or simply be not associated with the echo component anymore. ERLE, on the other hand, punishes each type of residual echo and also considers noise suppression effectiveness.

Efficiency analysis: Table 2 shows the memory footprint and complexity analysis³ of the methods studied in this work, entailing num-

³We used <https://pypi.org/project/torchinfo/>.

Table 1. ERLE in dB for the **STFE** condition, averaged over the respective 300 files of the test set.

LEC	Ours (Bark)	Ours (DFT)	DVQE-S[7]	DTLN[10]
37.57	60.10	<u>62.00</u>	40.00	68.78

Table 2. Efficiency analysis for the studied methods. Lowest demand is marked **bold** and second best results are underlined.

Attribute	Ours (Bark)	Ours (STFT)	DVQE-S[7]	DTLN[10]
Param (M)	1.58	2.04	0.72	3.16
MACs/s (M)	235.00	<u>240.00</u>	2170.00	408.00
RTF (%)	<u>0.22</u>	0.23	0.20	0.97

ber of multiply-accumulate operations per second (MACs/s), the number of trainable parameters, and the realtime factor (RTF), measured on an Intel i9-10850K CPU at 3.60 GHz. We observe that DVQE-S has the lowest parameter count and RTF, followed by our proposed Bark model. Both architectures prove realtime-capable on the tested CPU. However, since DVQE-S mainly consists of convolutional layers, way more MACs/s are required. In contrast, *our proposed fully connected model only requires about 10% of the DVQE-S models’ MACs/s*. Moreover, on a device like a speakerphone, efficiently implementing convolutional architectures is much more difficult than it is for fully connected ones. This means that RTF rankings can change significantly depending on the deployment platform. While our model has a higher parameter count than DVQE-S, the difference is not critical on modern devices. Combined with the previously reported good performance, *the low complexity of our model makes it a great fit for application in speakerphones.*

5. CONCLUSIONS

In this paper, we presented a realtime-capable joint acoustic echo control and noise reduction model for speakerphones, consisting of a linear echo canceller, followed by a lightweight neural network as postfilter. Our results demonstrated that the proposed design achieves an on-par or even improved performance compared to existing state-of-the-art solutions. An attractive trade-off between echo suppression and near-end speech preservation is offered along with a reasonable amount of model parameters. *Our proposed model excels all reference methods by far in computational complexity.*

6. REFERENCES

- [1] R. Cutler, Y. Hosseinkashi, J. Pool, S. Filipi, R. Aichner, Y. Tu, and J. Gehrke, “Meeting Effectiveness and Inclusiveness in Remote Collaboration,” *Proc. ACM Hum.-Comput. Interact.*, vol. 5, Apr. 2021.
- [2] E. Seidel, J. Franzen, M. Strake, and T. Fingscheidt, “Y²-Net FCRN for Acoustic Echo and Noise Suppression,” in *Proc. of Interspeech*, Brno, Czech Republic, Oct. 2021, pp. 4763–4767.
- [3] J. Franzen, E. Seidel, and T. Fingscheidt, “AEC in A Net-shell: On Target and Topology Choices for FCRN Acoustic Echo Cancellation,” in *Proc. of ICASSP*, Toronto, Canada, June 2021, pp. 156–160.
- [4] S. Braun and M. Valero, “Task Splitting for DNN-Based Acoustic Echo and Noise Removal,” in *Proc. of IWAENC*, Bamberg, Germany, Sept. 2022, pp. 386–390.

- [5] E. Seidel, R. Olsson, K. Haddad, Z. Li, P. Mowlae, and T. Fingscheidt, "Bandwidth-Scalable Fully Mask-Based Deep FCRN Acoustic Echo Cancellation and Postfiltering," in *Proc. of IWAENC*, Bamberg, Germany, Sept. 2022, pp. 406–410.
- [6] E. Seidel, P. Mowlae, and T. Fingscheidt, "Efficient Deep Acoustic Echo Suppression with Condition-Aware Training," in *Proc. of WASPAA*, New Paltz, NY, USA, Oct. 2023, pp. 1–5.
- [7] E. Indenbom, N. Ristea, A. Saabas, T. Parnamaa, J. Guzvín, and R. Cutler, "DeepVQE: Real Time Deep Voice Quality Enhancement for Joint Acoustic Echo Cancellation, Noise Suppression and Dereverberation," in *Proc. of Interspeech*, Dublin, Ireland, Aug. 2023, pp. 1–5.
- [8] Y. Liu, Y. Shi, Y. Li, K. Kalgaonkar, S. Srinivasan, and X. Lei, "SCA: Streaming Cross-Attention Alignment For Echo Cancellation," in *Proc. of ICASSP*, Rhodes Island, Greece, June 2023, pp. 1–5.
- [9] E. Indenbom, N. Ristea, A. Saabas, T. Parnamaa, and J. Guzvín, "Deep Model with Built-In Cross-Attention Alignment for Acoustic Echo Cancellation," *arXiv:2208.11308*, Aug. 2023.
- [10] N. L. Westhausen and B. T. Meyer, "Acoustic Echo Cancellation with the Dual-Signal Transformation LSTM Network," in *Proc. of ICASSP*, Toronto, Canada, June 2021, pp. 7138–7142.
- [11] H. Zhang and D. Wang, "Neural Cascade Architecture for Joint Acoustic Echo and Noise Suppression," in *Proc. of ICASSP*, Singapore, May 2022, pp. 671–675.
- [12] G. Enzner and P. Vary, "Frequency-Domain Adaptive Kalman Filter for Acoustic Echo Control in Hands-Free Telephones," *Signal Processing*, vol. 86, no. 6, pp. 1140–1156, June 2006.
- [13] K. Steinert, M. Schönle, C. Beaugeant, and T. Fingscheidt, "Hands-Free System with Low-Delay Subband Acoustic Echo Control and Noise Reduction," in *Proc. of ICASSP*, Las Vegas, NV, USA, Apr. 2008, pp. 1521–1524.
- [14] S. Panchapagesan, T. Z. Shabestary, and A. Narayanan, "On Training a Neural Residual Acoustic Echo Suppressor for Improved ASR," in *Proc. of Interspeech*, Dublin, Ireland, Aug. 2023, pp. 4019–4023.
- [15] L. Pfeifenberger, M. Zoehrer, and F. Pernkopf, "Acoustic Echo Cancellation with Cross-Domain Learning," in *Proc. of Interspeech*, Brno, Czech Republic, Oct. 2021, pp. 4753–4757.
- [16] E. Shachar, I. Cohen, and B. Berdugo, "Acoustic Echo Cancellation with the Normalized Sign-Error Least Mean Squares Algorithm and Deep Residual Echo Suppression," *Algorithms*, vol. 16, no. 3, Mar. 2023.
- [17] J.-M. Valin, S. Tanneti, K. Helwani, U. Isik, and A. Krishnaswamy, "Low-Complexity, Real-Time Joint Neural Echo Control and Speech Enhancement Based On Percepnet," in *Proc. of ICASSP*, Toronto, Canada, June 2021, pp. 7133–7137.
- [18] T. Haubner, M. Halimeh, A. Brendel, and W. Kellermann, "A Synergistic Kalman- and Deep Postfiltering Approach to Acoustic Echo Cancellation," in *Proc. of EUSIPCO*, Dublin, Ireland, Aug. 2021, pp. 990–994.
- [19] D. Yang, F. Jiang, W. Wu, X. Fang, and M. Cao, "Low-Complexity Acoustic Echo Cancellation with Neural Kalman Filtering," in *Proc. of ICASSP*, Rhodes Island, Greece, June 2023, pp. 1–5.
- [20] R. Cutler, A. Saabas, T. Parnamaa, M. Purin, E. Indenbom, N. Ristea, J. Guzvín, H. Gamper, S. Braun, and R. Aichner, "Acoustic Echo Cancellation Signal Processing Grand Challenge 2023," in *Proc. of ICASSP*, Rhodes Island, Greece, June 2023, pp. 1–5.
- [21] J.-M. Valin, U. Isik, N. Phansalkar, R. Giri, K. Helwani, and A. Krishnaswamy, "A Perceptually-Motivated Approach for Low-Complexity, Real-Time Enhancement of Fullband Speech," *arXiv:2008.04259*, Aug. 2020.
- [22] M. Harteneck, S. Weiss, and R.W. Stewart, "Design of Near Perfect Reconstruction Oversampled Filter Banks for Subband Adaptive Filters," *IEEE Transactions on Circuits and Systems II: Analog and Digital Signal Processing*, vol. 46, no. 8, pp. 1081–1085, Aug. 1999.
- [23] S. Ciochină, C. Paleologu, J. Benesty, and S. L. Grant, "An Optimized NLMS Algorithm for Acoustic Echo Cancellation," in *Proc. of ISSCS*, Iasi, Romania, July 2015, pp. 1–4.
- [24] S. Braun and I. Tashev, "Data Augmentation and Loss Normalization for Deep Noise Suppression," in *Speech and Computer*, Sept. 2020, pp. 79–86, Springer International Publishing.
- [25] P. Kabal, *An Examination and Interpretation of ITU-R BS.1387: Perceptual Evaluation of Audio Quality*, Ph.D. thesis, Department of Electrical Computer Engineering, McGill University, Dec. 2003.
- [26] A. Ephrat, I. Mosseri, O. Lang, T. Dekel, K. Wilson, A. Hassidim, W. T. Freeman, and M. Rubinstein, "Looking to Listen at the Cocktail Party: A Speaker-Independent Audio-Visual Model for Speech Separation," *ACM Trans. Graph.*, vol. 37, no. 4, July 2018.
- [27] S. Wisdom, J. R. Hershey, K. Wilson, J. Thorpe, M. Chinen, B. Patton, and R. A. Saurous, "Differentiable Consistency Constraints for Improved Deep Speech Enhancement," in *Proc. of ICASSP*, Brighton, UK, May 2019, pp. 900–904.
- [28] H. Dubey, A. Aazami, V. Gopal, B. Naderi, S. Braun, R. Cutler, A. Ju, M. Zohourian, M. Tang, H. Gamper, M. Golestaneh, and R. Aichner, "ICASSP 2023 Deep Noise Suppression Challenge," *arXiv:2303.11510*, Mar. 2023.
- [29] T. Ko, V. Peddinti, D. Povey, M. L. Seltzer, and S. Khudanpur, "A Study on Data Augmentation of Reverberant Speech for Robust Speech Recognition," in *Proc. of ICASSP*, New Orleans, LA, USA, Mar. 2017, pp. 5220–5224.
- [30] H. Zhang and D. Wang, "Neural Cascade Architecture for Multi-Channel Acoustic Echo Suppression," *IEEE/ACM Transactions on Audio, Speech, and Language Processing*, vol. 30, pp. 2326–2336, July 2022.
- [31] D. Kingma and J. Ba, "Adam: A Method for Stochastic Optimization," in *Proc. of ICLR*, San Diego, CA, USA, May 2015, pp. 1–15.
- [32] M. Purin, S. Sootla, M. Sponza, A. Saabas, and R. Cutler, "AECMOS: A Speech Quality Assessment Metric for Echo Impairment," in *Proc. of ICASSP*, Singapore, May 2022, pp. 901–905.
- [33] G. Enzner, H. Buchner, A. Favrot, and F. Kuech, "Acoustic Echo Control," in *Academic Press Library in Signal Processing*, vol. 4, pp. 807–877. Elsevier/Academic Press, 2013.
- [34] C. Reddy, V. Gopal, and R. Cutler, "DNSMOS P.835: A Non-Intrusive Perceptual Objective Speech Quality Metric to Evaluate Noise Suppressors," in *Proc. of ICASSP*, Singapore, May 2022, pp. 886–890.
- [35] R. Cutler, B. Nadari, M. Loide, S. Sootla, and A. Saabas, "Crowdsourcing Approach for Subjective Evaluation of Echo Impairment," in *Proc. of ICASSP*, Toronto, Canada, June 2021, pp. 406–410.